Published in final edited form as:
Phys Med Biol. 2008 February 21; 53(4): 925–935. doi:10.1088/0031-9155/53/4/007.

Vibration safety limits for magnetic resonance elastography

E C Ehman[1], **P J Rossman**[1], **S A Kruse**[1], **A V Sahakian**[2], and **K J Glaser**[1]

[1]Department of Radiology, Mayo Clinic, 200 First Street SW, Rochester, MN, 55905

[2]Department of Biomedical Engineering, McCormick School of Engineering and Applied Science, Northwestern University, 2145 Sheridan Rd., Evanston, IL 60208

Abstract

Magnetic resonance elastography (MRE) has been demonstrated to have potential as a clinical tool for assessing the stiffness of tissue in vivo. An essential step in MRE is the generation of acoustic mechanical waves within tissue via a coupled mechanical driver. Motivated by an increasing volume of human imaging trials using MRE, the objectives of this study were to audit the vibration amplitude of exposure for our IRB-approved human MRE studies, to compare these values to a conservative regulatory standard for vibrational exposure, and to evaluate the applicability and implications of this standard for MRE. MRE displacement data were examined from 29 MRE exams, including the liver, brain, kidney, breast, and skeletal muscle. Vibrational acceleration limits from a European Union directive limiting occupational exposure to whole-body and extremity vibrations (EU 2002/44/EC) were adjusted for time and frequency of exposure, converted to maximum displacement values, and compared to the measured in vivo displacements. The results indicate that the vibrational amplitudes used in MRE studies are below the EU whole-body vibration limit and the EU guidelines represent a useful standard that could be readily accepted by Institutional Review Boards to define standards for vibrational exposures for MRE studies in humans.

Keywords

Elastography; safety; vibration; MRI

1. Introduction

Magnetic resonance elastography (MRE) is an emerging diagnostic medical imaging technique for quantitatively assessing the viscoelastic properties of tissue (Muthupillai *et al* 1995, Muthupillai *et al* 1996). Many disease processes are characterized by marked changes in the mechanical stiffness of tissue, accounting for the diagnostic value of the traditional physical examination technique of palpation. Magnetic resonance elastography has been shown to have potential value in diverse applications, ranging from the diagnosis of cancer (McKnight *et al* 2002, Sinkus *et al* 2005) to assessing the biomechanical properties of skeletal muscle (Bensamoun *et al* 2006, Kruse *et al* 2000, Papazoglou *et al* 2005). One of the most promising diagnostic uses of MRE is for detecting and assessing hepatic fibrosis (Huwart *et al* 2006, Rouviere *et al* 2006).

A typical implementation of MR elastography is a three-step procedure involving (1) generating mechanical waves in the tissue of interest, (2) imaging the waves using a modified phase-contrast MRI technique, and (3) processing the wave images using an “inversion algorithm” to generate quantitative images depicting mechanical properties such as shear

glaser.kevin@mayo.edu, Phone: 507-284-9770, Fax: 507-284-9778.

stiffness (Muthupillai *et al* 1995, Muthupillai *et al* 1996). The mechanical waves employed in MRE are typically in the low acoustic frequency range of 40-150 Hz, and are often generated by a vibration device that is placed on the surface of the body over the region of interest. These devices must be designed so as not to create artefacts or electromagnetic noise and must be suitable for use in the high magnetic field of an MRI scanner. Investigators have described successful MRE driver devices that are based on electromechanical (Muthupillai *et al* 1995, Muthupillai *et al* 1996, Braun *et al* 2003), piezoelectric (Rossman *et al* 2003, Uffmann *et al* 2002), and remote pneumatic actuators (Vyacheslav *et al* 2006, Rossman *et al* 2006).

The MRI pulse sequences typically used for MRE have special motion-encoding gradients that are synchronized with the applied vibrations, resulting in remarkable sensitivity to the tiny cyclic tissue motions caused by propagating mechanical waves. Waves with amplitudes in the tens or hundreds of nanometres (less than the wavelength of light) can be imaged in living tissue with this technique (Muthupillai *et al* 1996). Most published in vivo applications of MRE have employed mechanical waves with displacement amplitudes in the tens of microns (Muthupillai *et al* 1995, Muthupillai *et al* 1996, McKnight *et al* 2002, Bensamoun *et al* 2006, Kruse *et al* 2000, Huwart *et al* 2006, Rouviere *et al* 2006).

Safety standards for static magnetic fields, time-varying gradients, and radiofrequency energy used in conventional MRI are well established (Kanal *et al* 2007, Marshall *et al* 2007) and are equally applicable to the imaging aspect of MRE. However, the safety of the applied mechanical vibrations is an additional issue that must be addressed by investigators in order to gain Institutional Review Board (IRB) approval for human research studies of MRE. This aspect of the technique is also relevant for regulatory and approval agencies of medical devices as MRE emerges as a clinical diagnostic imaging tool. Motivated by the increasing number of human imaging trials of MRE, the objective of this study was to audit the level of vibration exposure experienced by patients and volunteers in an IRB-approved human study of MRE and to evaluate the usefulness and applicability of an existing regulatory guideline for human vibration exposure in this regard.

2. Theory

The literature regarding the physiological impact of vibration exposure in humans is diverse. Exposure to extended periods of low-amplitude extremity or whole-body vibrations may be beneficial as a means to reduce bone loss (Rubin *et al* 2004) or muscle atrophy (Falempin and In-Albon 1999). However, exposure to acute, high-amplitude vibrations in the range of 32-250 Hz has been shown to temporarily reduce finger blood flow (Bovenzi *et al* 2000, Bovenzi *et al* 2004), and similar vibrations may affect muscle function and the neuromuscular system (Bosco *et al* 1999b, Bosco *et al* 1999a, Cardinale and Pope 2003, Cronin and Crewther 2004, Jackson and Turner 2003, Adamo *et al* 2002). Chronic occupational exposure to extremity and whole-body vibrations has been linked to an increased risk of hand-arm vibration syndrome (HAVS) (Bovenzi 1998a, 1998b, Necking *et al* 2004) and low-back pain (Bovenzi *et al* 1999). Of course all of the above vibrations are below the threshold for acute traumatic injury. Due to the above observations, standards have been developed to protect workers against overexposure (e.g., DHHS NIOSH Publication No. 89-106 (NIOSH 1989), ISO 5349 (ISO 2001a, 2001b), ISO 2631(ISO 1997), and EU Directive 2002/44/EC (EU 2002)). These guidelines have been used to assess and monitor occupational exposure to vibration and also to guide in the design of protective equipment.

In 2002, the European Parliament adopted Directive 2002/44/EC, which sets root-mean-squared (RMS) vibration exposure limits a_{lim} of 5 m/s^2 and 1.15 m/s^2 for extremity and whole-body “daily” 8-hour occupational exposures, respectively (EU 2002). The exposure limits are adjusted as defined in ISO standards 2631 (whole body) and 5349 (extremity) for duration and

frequency. The ISO standards define a number of frequency weighting curves that are to be applied to estimated RMS accelerations for different situations. The frequency weighting scheme in the ISO standards is very complicated, and also subject to some controversy (Griffin *et al* 2003,NIOSH 1989). In this work, a conservative weighting function is used that approximates the ISO 5349-2 weighting curve for extremity vibrations such that measured RMS accelerations a_{RMS} at frequencies above 16 Hz are multiplied by a weighting factor equal to 16/*f*, where *f* is the temporal frequency of the vibration, to yield frequency-weighted accelerations a_{hw}. Conversely, the limiting RMS acceleration a_{lim} is multiplied by a weighting factor equal to *f*/16 to yield a frequency-weighted maximum limit of acceleration $a_{\mathrm{hw},8}$.

Different durations of vibration exposure are weighted using an average energy method which assumes that the vibration dose at a greater amplitude but decreased duration would impart the same energy on the subject as the standard 8-hour dose described by the limits. The adjustment for durations other than 8 hours is as follows:

$$a_{\mathrm{hw},T}=a_{\mathrm{hw},8}\sqrt{\frac{8}{T}}, \tag{1}$$

where $a_{\mathrm{hw},T}$ is the maximum permissible acceleration for a duration of *T* hours. Therefore, the maximum RMS acceleration allowed by the EU standard for *T* hours of exposure at frequency *f* is

$$a_{\mathrm{hw},T}=a_{\mathrm{lim}}\left(\frac{f}{16}\right)\sqrt{\frac{8}{T}}, \tag{2}$$

where a_{lim} is 5 m/s^2 or 1.15 m/s^2 for extremity or whole-body vibrations, respectively.

Most MRE acquisition schemes yield quantitative measurements of local displacement amplitude. Since the EU directive provides vibration limits in terms of RMS acceleration, these limits must be converted to maximum displacement amplitudes to be directly comparable with MRE data. For a sinusoidal displacement of amplitude d_{max} and angular frequency $\omega = 2\pi f$, the displacement *x* at a time *t* is

$$x(t)=d_{\mathrm{max}}\sin(\omega t),\ \text{and}\ x_{\mathrm{RMS}}=\frac{d_{\mathrm{max}}}{\sqrt{2}}. \tag{3}$$

The instantaneous velocity of an element undergoing sinusoidal motion is related to the time derivative of the position function *x*(*t*):

$$v(t)=\frac{\mathrm{d}x(t)}{\mathrm{d}t}=\omega d_{\mathrm{max}}\cos(\omega t),\ \text{and}\ v_{\mathrm{RMS}}=\frac{\omega d_{\mathrm{max}}}{\sqrt{2}}. \tag{4}$$

Finally, the acceleration is related to the time derivative of the velocity function:

$$a(t)=\frac{\mathrm{d}v(t)}{\mathrm{d}t}=-\omega^2 d_{\max}\sin(\omega t),\ \text{and}\ a_{\mathrm{RMS}}=\frac{\omega^2 d_{\max}}{\sqrt{2}}. \tag{5}$$

From the previous equations, we can see that

$$d_{\max}=\frac{a_{\mathrm{RMS}}\sqrt{2}}{\omega^2}=\frac{a_{\lim}}{16\pi^2 f\sqrt{T}}. \tag{6}$$

The motion-encoding process and the calculation of the displacement amplitude of vibration for MRE have been described previously (Muthupillai *et al* 1996, Oliphant *et al* 2000, McCracken *et al* 2005, Rump *et al* 2007) and are summarized here. The vector displacement of tissue over time at position **r** is given by $\xi(\mathbf{r},t)$. The phase that is encoded into the transverse magnetization of the MR signal at **r** due to this motion occurring during the application of a magnetic field gradient $\mathbf{G}(t)$ is given by

$$\phi(\mathbf{r},\alpha)=\gamma\int_{-\infty}^{\infty}\mathbf{G}(t)\bullet\xi(\mathbf{r},t+\alpha)dt, \tag{7}$$

where α is an adjustable time delay (usually called a phase offset) between the source of the applied motion and motion-encoding gradient. When the motion-encoding gradient is applied along the direction x_i (where $x_1=x$, $x_2=y$, and $x_3=z$), then φ (now identified as φ_i) is a measure of the x_i component of the vector motion ξ:

$$\phi_i(\mathbf{r},\alpha)=\gamma\int_{-\infty}^{\infty}\mathbf{G}_i(t)\xi_i(\mathbf{r},t+\alpha)dt, \tag{8}$$

For the MRE data considered in this work, the applied motion is predominantly at one steady-state frequency F, and therefore the motion at every position **r** is assumed to be sinusoidal over time:

$$\xi_i(\mathbf{r},t+\alpha)=\xi_{i,0}(\mathbf{r})\bullet\sin(2\pi F(t+\alpha)), \tag{9}$$

where $\xi_{i,0}(\mathbf{r})$ is the amplitude of motion at **r**. The phase data φ_t are recorded at multiple phase offsets (usually 4-8) and then the Fourier transform over α is performed yielding the frequency-domain phase information Φ_i:

$$\Phi_i(\mathbf{r},f)=\gamma\Gamma_i^*(f)\Xi_i(\mathbf{r},f), \tag{10}$$

where $\mathbf{\Gamma}_t^*$ is the complex conjugate of the Fourier transform of the gradient function, and Ξ_t is the Fourier transform of the displacement. The magnitude of the Fourier transform of the phase information at **r** is therefore proportional to the magnitude of the Fourier transform of the displacement at **r**:

$$|\Phi_i(\mathbf{r}, f)| = \gamma \left|\Gamma_i^*(f)\right| \bullet |\Xi_i(\mathbf{r}, f)| . \tag{11}$$

Because the MRE data analyzed in this work were collected with the motion predominantly at one frequency F, the magnitude of the Fourier transforms of $\Phi_i(\mathbf{r}, f)$ and $\Xi_i(\mathbf{r}, f)$ at F yield the maximum amplitude of the corresponding sinusoidal signals $\varphi_i(\mathbf{r},t)$ and $\xi_i(\mathbf{r},t)$, which are $\varphi_{i,0}(\mathbf{r})$ and $\xi_{i,0}(\mathbf{r})$, respectively. The maximum displacement at $\mathbf{r}$ can then be calculated as

$$\xi_{i,0}(\mathbf{r}) = \frac{\phi_{i,0}(\mathbf{r})}{\gamma \left|\Gamma_i^*(F)\right|} = \frac{\pi F \phi_{i,0}(\mathbf{r})}{4\gamma N G_0}, \tag{12}$$

assuming a phase-difference acquisition involving N gradient pairs of a bipolar rectangular motion-encoding gradient with amplitude G_0 and frequency F.

3. Materials and Methods

Accumulating evidence suggests that MR elastography may be an effective method for detecting and assessing hepatic fibrosis, and a potential noninvasive alternative to biopsy for diagnosing this condition before it progresses to irreversible hepatic cirrhosis (Huwart *et al* 2006, Rouviere *et al* 2006). We chose this application for detailed review of vibrational exposure because it is becoming the first established clinical use of MRE. De-identified wave image data were retrospectively acquired from imaging datasets for 16 studies of patients and volunteers participating in an IRB-approved study of hepatic MRE. MRE has been well validated as a method for quantitatively assessing tissue vibration amplitudes and, in contrast to devices such as accelerometers, the technique provides noninvasive measurements of internal motion. All studies were performed using a 1.5 T whole-body imager (GE Medical Systems, Milwaukee, WI, USA). Subjects were imaged in the supine position with a 19-cm diameter passive vibrational driver placed against the anterior body wall. Continuous vibrations at 60 Hz were generated by a remotely situated active electromechanical driver device coupled to the passive driver by a flexible plastic tube (Rouviere *et al* 2006). Wave images were acquired in the axial plane with a 2D multislice SE-EPI MRE sequence (Yin *et al* 2006) with the following parameters: FOV = 32-42 cm, 2 shots, acquisition matrix = 96 × 96, receiver bandwidth = ±64 kHz, TR/TE = 1200/55 ms, 4 phase offsets, and 1 pair of 60-Hz trapezoidal motion-encoding gradients applied sequentially in 3 orthogonal directions. To achieve a final acquisition of 36 slices with an effective slice spacing of 5 mm using 10-mm thick spatial-spectral excitation pulses, two acquisitions were performed, each collecting 18 contiguous water-selective slices in 2 passes followed by 18 contiguous fat-selective slices in 2 passes. The two acquisitions for each chemical species were performed sequentially with the 18 slices prescribed for the second acquisition shifted by 5 mm with respect to the slices from the first acquisition. The fat and water images were combined by a simple weighted sum. The MRE acquisition time for these exams, and thus the exposure to the mechanical vibration, was less than 5 minutes.

In addition to the detailed review of vibration levels in the hepatic MRE application described above, we obtained representative datasets from 12 human MRE exams of healthy volunteers from IRB-approved studies of other parts of the body, including brain (40, 80, and 120 Hz; n=4), kidney (75 Hz; n=1), breast (90 Hz; n=2), and skeletal muscle (80, 90, and 100 Hz; n=5) (Dresner *et al* 2001, McKnight *et al* 2002, Kruse *et al* 2000, Rossman *et al* 2006, Yin *et al* 2006, McCracken *et al* 2005). The imaging parameters for these studies are listed in table 1. For the purpose of the calculations performed in this manuscript, the vibration exposure times

for all of these MRE exams was rounded up to 15 minutes of exposure. This is a conservative, but realistic approximation of the typical exposure time. The vibrational frequency selected for clinical applications of MRE depends on the properties of the tissue, the desired level of motion-encoding sensitivity, and the capabilities of the driver system. Higher frequencies provide shorter wavelengths and better resolution, but penetration into the body is limited by attenuation and viscoelastic effects more than at lower frequencies (Fung 1993). The frequencies used for clinical applications of MRE reflect this trade-off.

Wave data were processed using custom software developed for the inversion of MRE wave data (Manduca *et al* 2001, Grimm 2006). An ROI was drawn in the centre of the tissue under investigation from which the mean value of the magnitude signal was calculated. A threshold of 30% of this mean value was used to mask out low-signal portions of the image while retaining the majority of the tissue, including the subcutaneous fat for the liver exams. The mask was completed by drawing an elliptical ROI around the tissue and subcutaneous fat adjacent to the driver. The amplitude of vibration at each pixel was calculated from the wave data according to equation (12). This calculation was performed for each of the three orthogonally motion-encoded images and the total vector amplitude was calculated by taking the square root of the sum of squared component amplitudes. Vibration amplitude values across the entire cross section of the organ of interest were then compiled into a histogram and the maximum vibration amplitude for each dataset was defined as the 99^{th} percentile value of each histogram to reduce the sensitivity of the maximum amplitude measurement to residual noisy pixels. Median and maximum displacement amplitude values were calculated for each dataset.

4. Results

Figure 1 shows typical examples of MRE wave images from liver, brain, and breast acquisitions. The corresponding amplitude maps demonstrate a common characteristic of MRE data: high-amplitude motion at the periphery of each organ (near the source of the motion) and significant wave attenuation as the waves propagate deeper into the tissue. A typical displacement amplitude histogram for the hepatic MRE studies is shown in figure 2. The median amplitude value was approximately 26 μm, and the maximum (99^{th} percentile) amplitude value was 179 μm. At 60 Hz, this corresponds to an RMS frequency-weighted acceleration value of 18.0 m/s^2. A review of individual images confirmed that the maximum amplitude values occurred in the subcutaneous tissues adjacent to the driver rather than in the liver itself. Similar histogram profiles were observed for the representative datasets from the brain, breast, kidney, and skeletal muscle MRE studies. The calculated median and maximum amplitude values for all dataset groups are shown in table 2.

Figure 3 shows the result of frequency weighting the EU extremity and whole-body RMS acceleration exposure limits and adjusting them for a 15-minute exposure. The frequency weighting permits larger acceleration values at increasing frequencies. Figure 4 shows the maximum or peak displacement allowed under the EU directive. Because of the $1/\omega^2$ dependence of the displacement, the maximum displacement decreases with increasing frequency. The compiled displacement amplitude values for all of the assessed studies are also shown in figure 4 compared with the EU frequency-weighted maximum amplitude values.

5. Discussion and Conclusions

The results show that the average maximum tissue vibration amplitude observed in this sampling of hepatic MRE exams was approximately 200 μm, with most areas of the hepatic tissue experiencing considerably less vibration. These displacements were below the maximum displacement allowed using the EU directive as a guide. Similarly, for the other MRE applications surveyed, the maximum displacements were also below the EU limits. The

vibration levels applied to the patients and healthy volunteers in these studies were well tolerated by the subjects.

In the US, there are no Federal regulations which define maximum safe exposures to vibrations in diagnostic medical or occupational settings. Therefore, the IRB approval for the MRE examinations analyzed in this study was based on adherence to British Standard 6842 (BS 1987), as guided by the ISO 5349 (ISO 2001a,2001b) definitions for measuring and calculating accelerations for all anatomic regions except for head studies. For studies of the head and brain, the procedures prescribed by the ISO 2631 (ISO 1997) standards for whole-body vibration were used. The British Standard 6842 was recently replaced by ISO 5349-1. The current ISO standards outline procedures for measuring and assessing vibration exposure but do not recommend specific limits for exposure. More recently, the European Parliament adopted Directive 2002/44/EC (EU 2002). The stated goal of this directive was to provide a clear and concise set of limits for occupational vibrational exposure that would serve as a minimum requirement for all member states. This directive sets specific values for vibration exposure limits and uses the ISO standards as guidelines for the assessment of vibration exposure. As with x-ray exposure, the exposure of patients to vibration for diagnostic purposes must be considered on the basis of medical considerations and individual benefit versus risk. The availability of an accepted standard for chronic occupational vibration exposure provides a reasonable starting point for this process.

The goal of this work was to identify a suitable guideline for maximum vibration exposure in clinical applications of MRE that would be (1) conservative in terms of any potential risk to the subject, (2) straightforward to monitor and assess, and (3) have reasonable justification for institutional IRBs and regulatory agencies. The choice of the EU whole-body exposure limit with the time and frequency weightings presented here as an upper bound for MRE vibration exposure meets all three of these requirements.

The EU whole-body exposure limit was selected as a target in this study because it is more conservative than the EU extremity limit. However, MRE vibration exposures rarely meet the definition of whole-body vibration, since MRE vibrations are typically applied locally. The choice in this work of performing calculations based on a 15-minute exposure is also conservative based on current clinical MRE protocols. Current 2D MRE acquisitions can be performed in 5 minutes or less, while the desire for 3D MRE data may push future MRE exams closer to the realm of 15-minute acquisition times depending on the acquisition strategy.

The MRE wave images demonstrate that the highest vibration amplitudes are typically measured in the cutaneous and subcutaneous tissues adjacent to the driver. Vibrational amplitudes in the deeper tissues and organs that are the focus of clinical imaging are greatly attenuated. The results of this study have demonstrated that when sufficient driver power is used to provide diagnostically suitable wave amplitudes for MRE in deep tissues, the vibrational exposure of tissues located adjacent to the driver are still within the proposed guidelines. This approach of limiting vibration exposure based on the maximum value observed near the surface is likely to be overconservative, because skin and subcutaneous tissues are probably designed through evolution to handle external mechanical energy from the environment to shield deeper structures. In the future, it may be more appropriate to develop a standard that refers to vibration amplitudes in target organs or to a spatially averaged vibrational dose. This would substantially raise the vibration amplitudes that would be permitted within the guideline.

In conclusion, the results indicate that the typical vibrational displacements used in current human MRE studies are below the values that would be permitted by even the conservative EU whole-body vibration standard. We conclude that the EU Directive 2002/44/EC represents

a useful standard at the conservative end of the spectrum that should be readily accepted by Institutional Review Boards for defining maximum vibrational amplitudes that can be used for MRE in humans.

Acknowledgments

This work was supported by NIH grants EB 001981, CA 91959, and EB 00812.

References

Adamo DE, Martin BJ, Johnson PW. Vibration-induced muscle fatigue, a possible contribution to musculoskeletal injury. Eur J Appl Physiol 2002;88:134–40. [PubMed: 12436281]

Bensamoun SF, Ringleb SI, Littrell L, Chen Q, Brennan M, Ehman RL, An KN. Determination of thigh muscle stiffness using magnetic resonance elastography. J Magn Reson Imaging 2006;23:242–7. [PubMed: 16374878]

Bosco C, Cardinale M, Tsarpela O. Influence of vibration on mechanical power and electromyogram activity in human arm flexor muscles. Eur J Appl Physiol 1999a;79:306–11.

Bosco C, Colli R, Introini E, Cardinale M, Tsarpela O, Madella A, Tihanyi J, Viru A. Adaptive responses of human skeletal muscle to vibration exposure. Clin Physiol 1999b;19:183–7. [PubMed: 10200901]

Bovenzi M. Exposure-response relationship in the hand-arm vibration syndrome: an overview of current epidemiology research. Int Arch Occup Environ Health 1998a;71:509–19. [PubMed: 9860158]

Bovenzi M. Vibration-induced white finger and cold response of digital arterial vessels in occupational groups with various patterns of exposure to hand-transmitted vibration. Scand J Work Environ Health 1998b;24:138–44. [PubMed: 9630062]

Bovenzi M, Lindsell CJ, Griffin MJ. Magnitude of acute exposures to vibration and finger circulation. Scand J Work Environ Health 1999;25:278–84. [PubMed: 10450780]

Bovenzi M, Lindsell CJ, Griffin MJ. Acute vascular responses to the frequency of vibration transmitted to the hand. Occup Environ Med 2000;57:422–30. [PubMed: 10810133]

Bovenzi M, Welsh AJ, Griffin MJ. Acute effects of continuous and intermittent vibration on finger circulation. Int Arch Occup Environ Health 2004;77:255–63. [PubMed: 15034718]

Braun J, Braun K, Sack I. Electromagnetic actuator for generating variably oriented shear waves in MR elastography. Magn Reson Med 2003;50:220–2. [PubMed: 12815700]

BS. Measurement and evaluation of human exposure to vibration transmitted to the hand, BS 6842. London: British Standards Institution; 1987.

Cardinale M, Pope MH. The effects of whole body vibration on humans: dangerous or advantageous. Acta Physiol Hung 2003;90:195–206. [PubMed: 14594190]

Cronin J, Crewther B. Training volume and strength and power development. J Sci Med Sport 2004;7:144–55. [PubMed: 15362310]

Dresner MA, Rose GH, Rossman PJ, Muthupillai R, Manduca A, Ehman RL. Magnetic resonance elastography of skeletal muscle. J Magn Reson Imaging 2001;13:269–76. [PubMed: 11169834]

EU. Directive 2002/44/EC of the European Parliament and of the Council of 25 June 2002 on the minimum health and safety requirements regarding the exposure of workers to the risks arising from physical agents (vibration) (sixteenth individual Directive within the meaning of Article 16(1) of Directive 89/391/EEC) - Joint Statement by the European Parliament and the Council. Luxembourg: European Union; 2002.

Falempin M, In-Albon SF. Influence of brief daily tendon vibration on rat soleus muscle in non-weight-bearing situation. J Appl Physiol 1999;87:3–9. [PubMed: 10409551]

Fung, YC. Biomechanics: mechanical properties of living tissues. New York: Springer-Verlag; 1993.

Griffin M, Bovenzi M, Nelson C. Dose-response patterns for vibration-induced white finger. Occup Environ Med 2003;60:16–26. [PubMed: 12499452]

Grimm, R. MR acquisition techniques for dynamic MR elastography. ISMRM Flow and Motion Workshop; New York, NY. 2006.

Huwart L, Peeters F, Sinkus R, Annet L, Salameh N, ter Beek LC, Horsmans Y, Van Beers BE. Liver fibrosis: non-invasive assessment with MR elastography. NMR Biomed 2006;19:173–9. [PubMed: 16521091]

ISO. Mechanical vibration and shock -- Evaluation of human exposure to whole-body vibration -- Part 1: General requirements, ISO 2631-1:1997. Geneva: International Organization for Standardization; 1997.

ISO. Mechanical vibration -- Measurement and evaluation of human exposure to hand-transmitted vibration -- Part 1: General requirements, ISO 5349-1:2001. Geneva: International Organization for Standardization; 2001a.

ISO. Mechanical vibration -- Measurement and evaluation of human exposure to hand-transmitted vibration -- Part 2: Practical guidance for measurement at the workplace, ISO 5349-2:2001. Geneva: International Organization for Standardization; 2001b.

Jackson SW, Turner DL. Prolonged muscle vibration reduces maximal voluntary knee extension performance in both the ipsilateral and the contralateral limb in man. Eur J Appl Physiol 2003;88:380–6. [PubMed: 12527966]

Kanal E, Barkovich AJ, Bell C, Borgstede JP, Bradley WG Jr, Froelich JW, Gilk T, Gimbel JR, Gosbee J, Kuhni-Kaminski E, Lester JW Jr, Nyenhuis J, Parag Y, Schaefer DJ, Sebek-Scoumis EA, Weinreb J, Zaremba LA, Wilcox P, Lucey L, Sass N, the ACR Blue Ribbon Panel on MR Safety. ACR Guidance Document for Safe MR Practices: 2007. AJR Am J Roentgenol 2007;188:1447–74. [PubMed: 17515363]

Kruse SA, Smith JA, Lawrence AJ, Dresner MA, Manduca A, Greenleaf JF, Ehman RL. Tissue characterization using magnetic resonance elastography: preliminary results. Phys Med Biol 2000;45:1579–90. [PubMed: 10870712]

Manduca A, Oliphant TE, Dresner MA, Mahowald JL, Kruse SA, Amromin E, Felmlee JP, Greenleaf JF, Ehman RL. Magnetic resonance elastography: non-invasive mapping of tissue elasticity. Med Image Anal 2001;5:237–54. [PubMed: 11731304]

Marshall J, Martin T, Downie J, Malisza K. A comprehensive analysis of MRI research risks: in support of full disclosure. The Canadian Journal of Neurological Sciences 2007;34:11–7. [PubMed: 17352342]

McCracken PJ, Manduca A, Felmlee J, Ehman RL. Mechanical transient-based magnetic resonance elastography. Magn Reson Med 2005;53:628–39. [PubMed: 15723406]

McKnight AL, Kugel JL, Rossman PJ, Manduca A, Hartmann LC, Ehman RL. MR elastography of breast cancer: preliminary results. AJR Am J Roentgenol 2002;178:1411–7. [PubMed: 12034608]

Muthupillai R, Lomas DJ, Rossman PJ, Greenleaf JF, Manduca A, Ehman RL. Magnetic resonance elastography by direct visualization of propagating acoustic strain waves. Science 1995;269:1854–7. [PubMed: 7569924]

Muthupillai R, Rossman PJ, Lomas DJ, Greenleaf JF, Riederer SJ, Ehman RL. Magnetic resonance imaging of transverse acoustic strain waves. Magn Reson Med 1996;36:266–74. [PubMed: 8843381]

Necking LE, Lundborg G, Lundstrom R, Thornell LE, Friden J. Hand muscle pathology after long-term vibration exposure. J Hand Surg [Br] 2004;29:431–7.

NIOSH. Occupational Exposure to Hand-Arm Vibration, No 89-106. Cincinnati, OH: National Institute for Occupational Safety and Health, US Department of Health and Human Services; 1989.

Oliphant, TE.; Ehman, RL.; Greenleaf, JF. Magnetic resonance elastography revisited: reinterpreting phase-difference data as the output of a linear filter. 8th Proc Int Soc Magn Reson Med; Denver, Colorado. 2000.

Papazoglou S, Braun J, Hamhaber U, Sack I. Two-dimensional waveform analysis in MR elastography of skeletal muscles. Phys Med Biol 2005;50:1313–25. [PubMed: 15798324]

Rossman, PJ.; Glaser, KJ.; Felmlee, JP.; Ehman, RL. Piezoelectric bending elements for use as motion actuators in MR elastography. 11th Proc Int Soc Magn Reson Med; Toronto, Ontario, Canada. 2003.

Rossman, PJ.; Kruse, SA.; Hulshizer, T.; Ehman, RL. Pneumatically actuated driver for use in MRE of the brain. ISMRM Flow and Motion Workshop; New York, NY. 2006.

Rouviere O, Yin M, Dresner MA, Rossman PJ, Burgart LJ, Fidler JL, Ehman RL. MR elastography of the liver: preliminary results. Radiology 2006;240:440–8. [PubMed: 16864671]

Rubin C, Recker R, Cullen D, Ryaby J, McCabe J, McLeod K. Prevention of postmenopausal bone loss by a low-magnitude, high-frequency mechanical stimuli: a clinical trial assessing compliance, efficacy, and safety. J Bone Miner Res 2004;19:343–51. [PubMed: 15040821]

Rump J, Klatt D, Braun J, Warmuth C, Sack I. Fractional encoding of harmonic motions in MR elastography. Magn Reson Med 2007;57:388–95. [PubMed: 17260354]

Sinkus R, Tanter M, Xydeas T, Catheline S, Bercoff J, Fink M. Viscoelastic shear properties of in vivo breast lesions measured by MR elastography. Magn Reson Imaging 2005;23:159–65. [PubMed: 15833607]

Uffmann K, Abicht C, Grote W, Quick HH, Ladd ME. Design of an MR-compatible piezoelectric actuator for MR elastography. Concept Magnetic Res 2002;15:239–54.

Vyacheslav, K.; Rossman, PJ.; Ehman, RL. Passive array mechanical driver for magnetic resonance elastography of the breast. 14th Proc Int Soc Magn Reson Med; Seattle, WA. 2006.

Yin, M.; Rossman, PJ.; Manduca, A.; Ehman, RL. MR elastography of abdominal organs. ISMRM Flow and Motion Workshop; New York, NY. 2006.

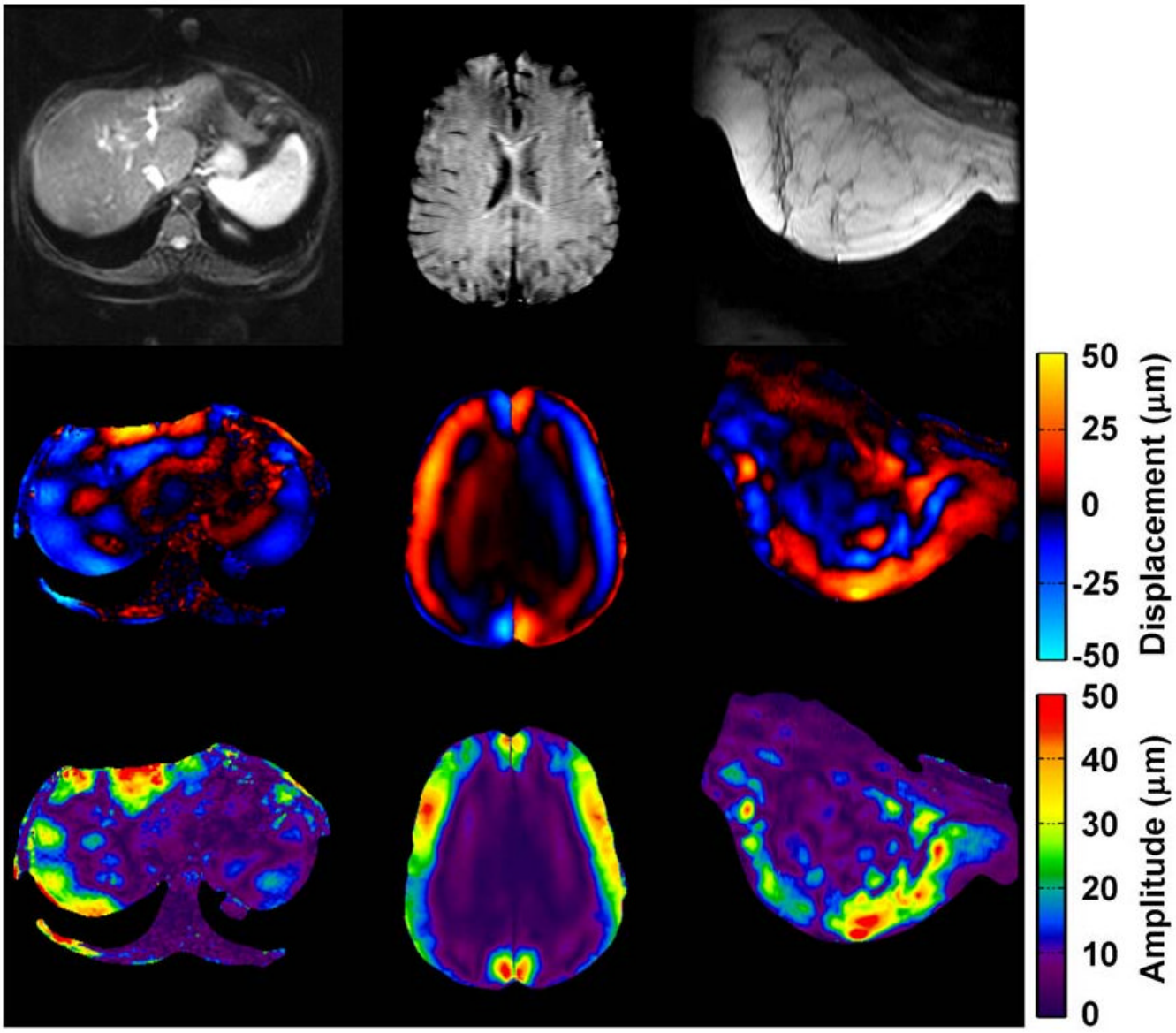

Figure 1.
From left to right, example MRE magnitude images (top), wave images (middle), and resulting displacement amplitude maps (bottom) for liver (60 Hz), brain (80 Hz), and breast (90 Hz) MRE exams. The motion-encoding gradient direction is through-plane for the liver and breast cases, and is up-down for the brain case.

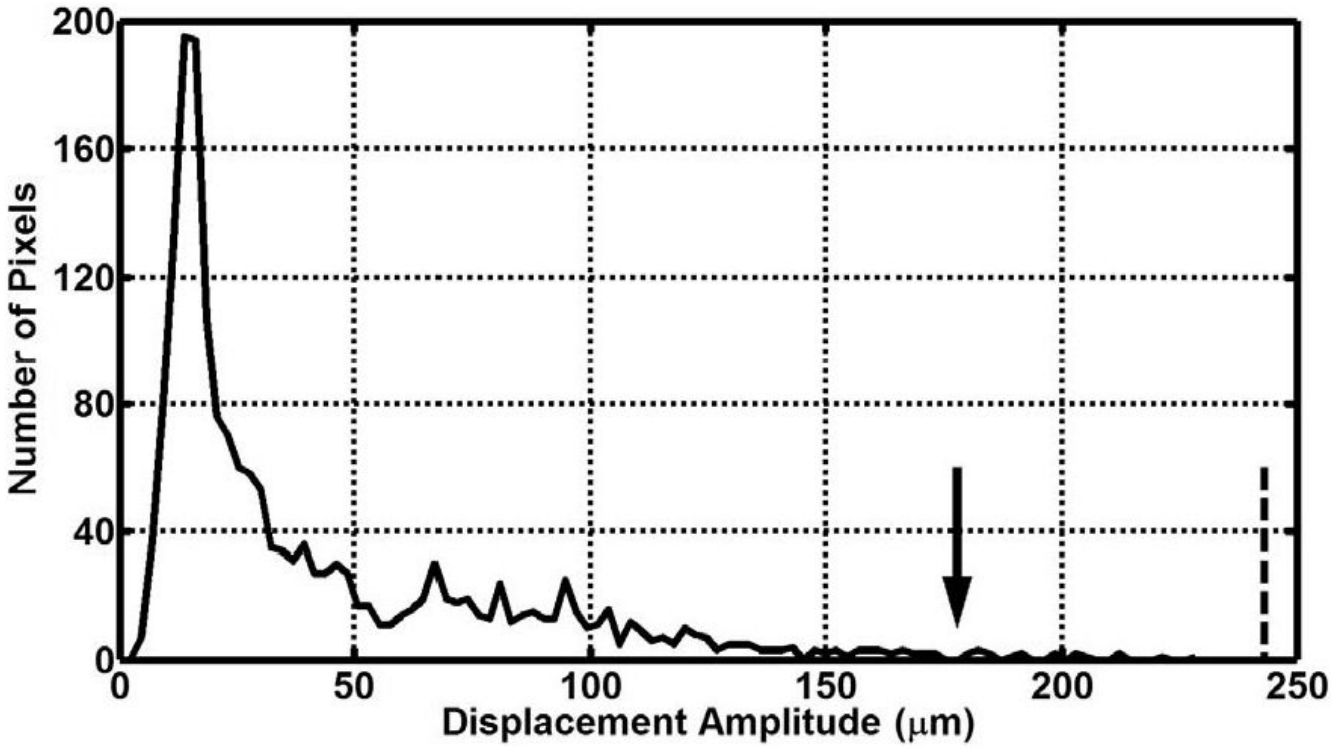

Figure 2.
Example histogram of liver displacement amplitude data. The arrow denotes the displacement amplitude greater than 99% of pixels (179 μm). The dotted line shows the maximum allowable whole-body displacement as prescribed by the EU 2002 standard for a 15-minute exposure (243 μm)

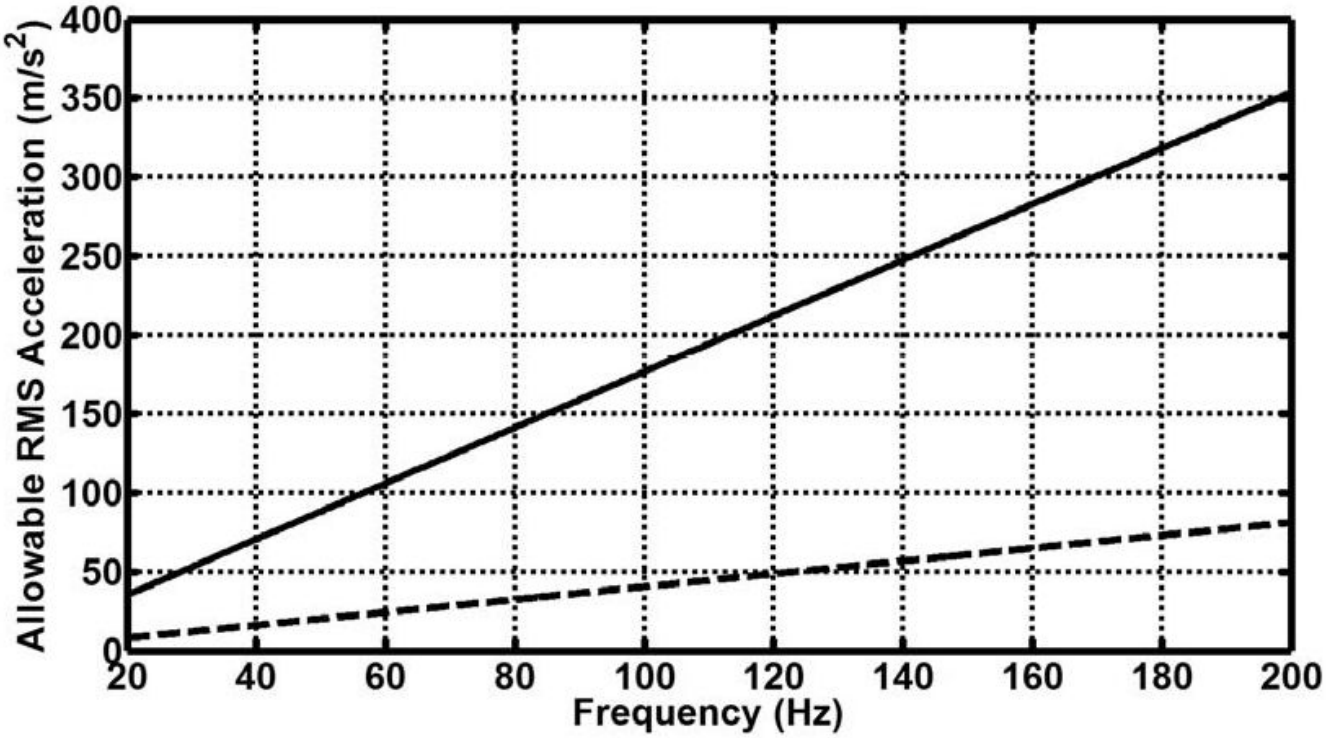

Figure 3.
Frequency-weighted maximum permissible acceleration ($a_{hw,T}$) according to the EU whole-body and extremity vibration limits for a 15-minute exposure. The dotted line shows the whole-body limit, while the sold line shows the extremity limit.

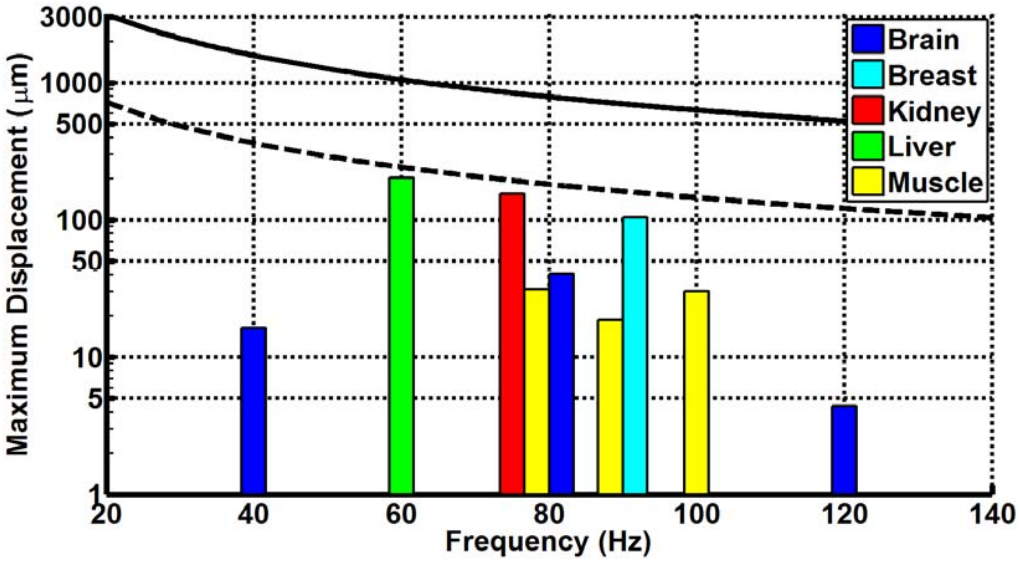

Figure 4.

Frequency-weighted maximum permissible displacement (d_{max}) according to the EU whole-body and extremity vibration limits for a 15-minute exposure. The dotted line shows the whole-body limit, while the sold line shows the extremity limit. The colored bars denote the experimentally determined mean maximum amplitudes in the MRE exams of liver, brain, breast, kidney, and muscle at various frequencies. Note the logarithmic scale on the displacement axis to account for the order-of-magnitude difference between typical MRE displacement amplitudes and the EU limits.

Table 1

Imaging parameters of various MRE exams surveyed in which full vector wave motion was obtained.

Parameters	Liver	Brain	Kidney	Breast	Skeletal Muscle
Sequence	2D SE EPI	2D GRE	2D GRE	2D GRE	2D GRE
FOV	32-42 cm	20-24 cm	24	16-20 cm	16-24 cm
Matrix	96×96	256×64	256×64	256×64	256×64
Shots/Flip Angle	2 shots	60°	30°	60°	45°
Slice Thickness	10 mm	5 mm	5 mm	5 mm	5 mm
Phase Offsets	4	8	4	4	8
Frequency	60 Hz	40,80,120 Hz	75 Hz	90 Hz	80,90,100 Hz
TR/TE	1200/55 ms	200/44 ms	60/24 ms	150/22 ms	100/23 ms
Driver Type	Passive Drum	EM coil	Passive Drum	EM coil	Passive Tube
Acquisition Time	< 5 min	10.24 min	1.50 min	3.84 min	5.12 min

Table 2

Excitation frequency, number of studies examined, mean displacement amplitude, and maximum displacement amplitude values for each anatomic region studied.

Anatomic Region Imaged	Excitation Frequency (Hz)	Number of Studies Compiled	Mean of Median Displacement Values (μm)	Mean of Maximum Displacement Values (μm)
Brain	40	1	7.33	16.40
Brain	80	2	4.67	40.45
Brain	120	1	2.70	4.37
Breast	90	2	21.3	104.10
Kidney	75	1	21.18	154.04
Liver	60	16	43.03	202.49
Muscle	80	2	2.16	31.11
Muscle	90	1	1.18	18.59
Muscle	100	2	2.91	30.15